

## A facile synthesis of single-crystal mullite nanobelts†

Bing Zhang,<sup>a,b</sup> Chuanbao Cao,<sup>\*a</sup> Xu Xiang<sup>a</sup> and Hesun Zhu<sup>a</sup><sup>a</sup> Research Center of Materials Science, Beijing Institute of Technology, Beijing 100081, People's Republic of China. E-mail: cbcao@bit.edu.cn<sup>b</sup> Building Materials Research Center of Henan Province, Zhengzhou 450002, People's Republic of China

Received (in Cambridge, UK) 16th June 2004, Accepted 31st August 2004

First published as an Advance Article on the web 24th September 2004

Single-crystal mullite nanobelts were prepared by a simple sol-gel method using  $\text{WO}_3$  as a catalyst. The nanobelts are straight and uniform with a width of 200 nm and length of 3–4  $\mu\text{m}$ .

The fabrication of one-dimensional nanomaterials, such as nanotubes, nanowires, nanorods, and nanobelts, has received considerable attention owing to their potential for a number of important applications in electronic and photonic nanodevices, biotechnology as well as nanostructure composite materials.<sup>1,2</sup> Ceramics with their unique physical properties offer great potential for future device developments. But fabrication of artificial nanostructured ceramic materials has been recognized as hard to attain due to their multicomponents and high temperature synthetic strategy.<sup>3</sup> Mullite ( $3\text{Al}_2\text{O}_3 \cdot 2\text{SiO}_2$ ) is the only intermediate stable compound in the  $\text{Al}_2\text{O}_3$ – $\text{SiO}_2$  system and it is an important ceramic material for electronic, optical, and high-temperature structure applications.<sup>4,5</sup> The low coefficient of thermal expansion (CTE), low density and low thermal conductivity of mullite make it useful for optical applications as mid-infrared windows.<sup>6</sup> Its low dielectric constant and dielectric loss, coupled with a smaller CTE mismatch to silicon than  $\text{Al}_2\text{O}_3$  also make it a valuable material for use in microelectronics packaging and substrates.<sup>3,5</sup> Mullite fiber is also an important component in reinforced composites owing to its higher oxidation resistance than non-oxide fibers.<sup>7,8</sup> To the best of our knowledge, mullite nanobelts or nanorods have not been synthesized to date.

In this communication we present a facile process for preparing mullite nanobelts or nanorods by a sol-gel method, in which  $\text{WO}_3$  was used as a catalyst. Commercially available aluminium chloride ( $\text{AlCl}_3$ ) and tetraethoxysilane (TEOS) were used as the source materials for making the gel precursor. Ammonium meta-tungstate hydrate was employed as catalyst source of  $\text{WO}_3$ . The relative molar composition of the source materials was  $\text{AlCl}_3/\text{TEOS}/\text{H}_2\text{O} = 3 : 1 : 120$  and the molar ratio of  $\text{WO}_3/\text{AlCl}_3$  was 1 : 6. These source solutions and the catalyst were mixed and stirred at 60 °C for 4 h, a creamy white-green gel was formed. The gel was transferred into an aluminium boat, and baked at 200 °C for 10 h. The aluminium boat was placed into a tube furnace and heated at a rate of 10 °C/min up to 1200 °C. The reaction was kept at 1200 °C for 5 h and then cooled naturally to room temperature. White products were obtained.

The morphology and structure of the products have been examined by X-ray diffraction (XRD, D/Max-III, Japan), scanning electron microscopy (SEM, Hitachi S-3500), energy dispersive X-ray spectroscopy (EDS), transmission electron microscopy (TEM, Hitachi H-800), and electron diffraction (ED).

The X-ray diffraction (XRD) pattern of as-synthesized products is shown in Fig. 1. All diffraction peaks can be perfectly indexed to the orthorhombic mullite structure. The mullite lattice constants calculated from the XRD data are  $a = 0.756$  nm,  $b = 0.770$  nm,  $c = 0.288$  nm, which is in good agreement with the reported data (JCPDS No. 15-0776).

The SEM image shows the general morphology of the mullite nanobelts (Fig. 2). Fig. 2(A) reveals that the synthesized products

consist of abundant nanobelts. Fig. 2(B) shows that the nanobelts are usually very straight with uniform width of 200 nm and length of up to 3–4  $\mu\text{m}$ . The thickness is about 20 nm, which was measured during the SEM observation. The EDS spectra reveal that the nanobelt is composed of Al, Si and O, and the atomic ratio of Al to Si, within the experimental limit, is close to 3 : 1, which is in agreement with the ratio of mullite compositions. There was no detectable tungsten in the nanobelts (the detection limit is  $\sim 2$  at%), which is attributed to the evaporation of  $\text{WO}_3$  above 1150 °C.<sup>9,10</sup>

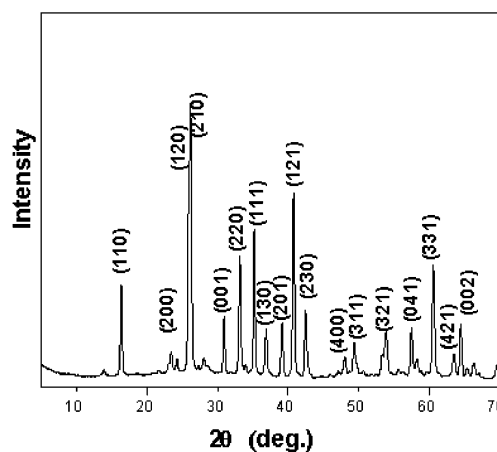


Fig. 1 XRD pattern of the as-synthesized nanobelts.

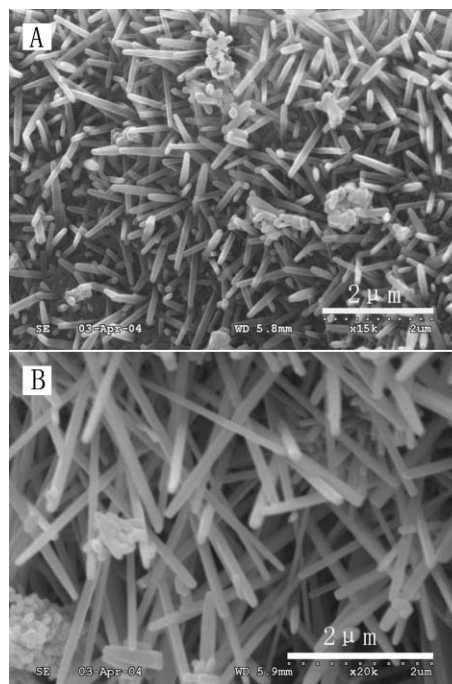
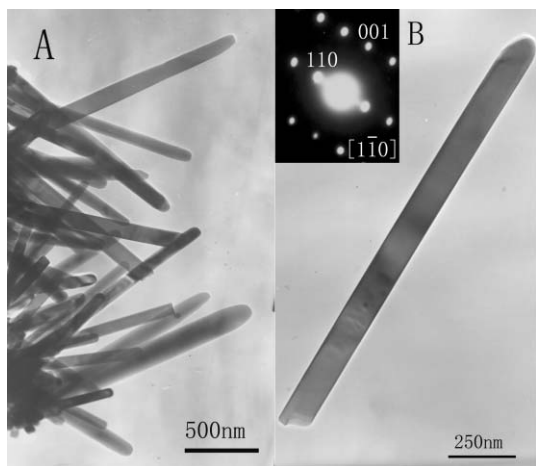
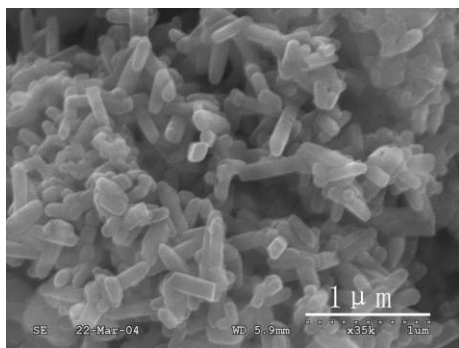


Fig. 2 SEM images of the mullite. (A) Typical top image. (B) Typical side image.

† Electronic supplementary information (ESI) available: Figs. 1S–3S. See <http://www.rsc.org/suppdata/cc/b4/b409087j/>



**Fig. 3** TEM image of mullite nanobelts (A), TEM image of a mullite single belt and the corresponding electron diffraction pattern [110] (B).



**Fig. 4** SEM image of the mullite precursors calcined at 1000 °C for 5 h.

Fig. 3 shows the TEM results of the as-prepared mullite nanobelts. Fig. 3(A) is a TEM image of representative mullite nanobelts. The nanobelts are straight and have a smooth surface. Fig. 3(B) is a TEM image of a single belt, together with the SAED pattern (insert picture). The SAED pattern can be indexed to the orthorhombic mullite structure and also indicates that the mullite nanobelt is a single crystal. The analysis of the SAED pattern shows that the growth direction of the mullite nanobelts is [001].

Further experimental results (Fig. 1S) indicated that under the same conditions, in the absence of  $\text{WO}_3$ , only particles of mullite were observed, and the nanobelts became nanorods with a rectangular section when the molar ratio of  $\text{WO}_3/\text{AlCl}_3 = 1 : 6$  was elevated to  $1 : 2$ . So the catalyst of  $\text{WO}_3$  plays an important role in the morphology of the products. There is a strong correlation between the synthesis of nanobelts and the presence of  $\text{WO}_3$ .

Mullite is a unique family of oxide structures and belongs to the aluminium silicate family with an orthorhombic structure. The mullite crystal structure consists of a three-dimensional framework of alternate corner-sharing among the  $\text{AlO}_6$  octahedra and the  $\text{SiO}_4$  (or  $\text{AlO}_4$ ) tetrahedra. The aluminium silicate crystal structure can be modified into various orthorhombic structures, ranging from sillimanite  $\text{Al}_2\text{O}_3 \cdot \text{SiO}_2$  to  $4\text{Al}_2\text{O}_3 \cdot \text{SiO}_2$  achieved by substituting  $\text{Si}^{4+}$  ions with  $\text{Al}^{3+}$  ions in the tetrahedral sites of the alternating aluminium and silicon columns.<sup>11</sup> When  $\text{WO}_3$  was added to a mullite precursor, it reacted with alumina first to form aluminium tungstate,  $\text{Al}_2\text{O}_3 \cdot 3\text{WO}_3$ , which is confirmed to exist at a low temperature of 1000 °C by our XRD result (Fig. 2S), and finally to transform the mullite phase. The crystal structure of aluminium tungstate ( $\text{Al}_2\text{O}_3 \cdot 3\text{WO}_3$ ) (JCPDS No. 81-2415) has

orthorhombic symmetry and consists of a three-dimensional framework of corner-linked  $\text{AlO}_6$  octahedra and  $\text{WO}_4$  tetrahedra alternately.<sup>12-14</sup> Tungstates or  $\text{WO}_3$  easily form one-dimensional structures, they have a strong tendency to grow an anisotropic structure.<sup>14-17</sup> Fig. 4 shows that some rod-like grains formed after the mullite precursors were calcined at 1000 °C for 5 h. The EDS results (Fig. 3S) show that the rod-like precursor is composed of Al, W and O elements, the most common atomic ratio of Al/W is close to 2 : 2.9. The EDS results together with the XRD result could prove that the precursor of  $\text{Al}_2\text{O}_3 \cdot 3\text{WO}_3$  had formed. Based on similarities between mullite and aluminium tungstate in crystal structure and their anisotropic tendency, it is reasonable to propose that after adding  $\text{WO}_3$ , one-dimensional aluminium tungstate formed first, acted as an epitaxial template, and induced the mullite to grow one-dimensional material. During the growth of the mullite nanobelt, the octahedral  $\text{AlO}_6$  chain is aligned in the *c*-direction and cross linked by  $\text{SiO}_4$  and  $\text{AlO}_4$  tetrahedra,<sup>11,18</sup> so the mullite nanobelts are *c*-axis oriented and easily grow along the direction of [001], which is consistent with our SAED pattern result. Further study is being performed to clarify the mechanism of mullite nanobelt formation and the present method would be a promising way to prepare other aluminate ceramic nanobelts or nanorods.

In summary, large-scale synthesis of single-crystal mullite nanobelts has been successfully realized for the first time by a simple sol-gel method using  $\text{WO}_3$  as a catalyst. The catalyst of  $\text{WO}_3$  plays an important role in the growth of mullite nanobelts. Because of mullite's excellent mechanical, thermal and chemical properties, mullite nanobelts are promising candidates for the reinforcing element in ceramic-, metal-, and polymer-matrix composites. Compared with the bulk or fibres of mullite, single-crystal mullite nanobelts with a smooth surface are also promising substrates for nanoelectronics in the future.

We thank the Research Foundation for the Doctoral Program of Higher Education of China (Grant No. 20020007029) and BIT basic research foundation for financial support.

## Notes and references

- J. Jiang, L. L. Henry, K. L. Gnanasekar, C. Chonglin and E. I. Meletis, *Nano Lett.*, 2004, **4**, 741.
- X. Wang and Y. D. Li, *Chem. Commun.*, 2002, 764.
- R. Barnwal, M. P. Villar, R. Garcia and M. Laine, *J. Am. Ceram. Soc.*, 2001, **84**, 951.
- M. A. Camerucci, G. Urretavizcaya, M. S. Castro and A. L. Cavalieri, *J. Eur. Ceram. Soc.*, 2001, **21**, 2917.
- R. R. Tummala, *J. Am. Ceram. Soc.*, 1991, **74**, 895.
- I. A. Aksay, D. M. Dabbs and M. Sarikaya, *J. Am. Ceram. Soc.*, 1991, **74**, 2343.
- V. Valcarcel, A. Souto and F. Guitian, *Adv. Mater.*, 1998, **10**, 138.
- L. H. Kong, J. Ma and H. Huang, *Adv. Eng. Mater.*, 2002, **4**, 490.
- I. Nikovo, V. Nikovo, D. Kovacheva and P. Peshev, *J. Alloys Compd.*, 2003, **351**, 289.
- A. Dabkowski, H. A. Dabkowska, J. E. Greedan, G. Adachi, Y. Kobayashi, S. Tamura, M. Hiraiwa and N. Imanaka, *J. Cryst. Growth*, 1999, **197**, 879.
- X. Y. Kong, Z. L. Wang and J. Wu, *Adv. Mater.*, 2003, **15**, 1445.
- J. S. O. Evans, T. A. Mary and A. W. Sleight, *J. Solid State Chem.*, 1997, **133**, 580.
- N. Imanaka, M. Hiraiwa, G. Adachi, H. Dabkowska and A. Dabkowska, *J. Cryst. Growth*, 2000, **220**, 176.
- S. H. Yu, B. Liu, M. S. Mo, J. H. Huang, X. M. Liu and Y. T. Qian, *Adv. Funct. Mater.*, 2002, **12**, 219.
- Z. H. Liu, Y. Bando and C. C. Tang, *Appl. Phys. Lett.*, 2003, **372**, 179.
- Y. B. Li, Y. Bando, D. Golberg and K. Kurashima, *Appl. Phys. Lett.*, 2003, **367**, 214.
- H. Qi, C. Y. Wang and J. Liu, *Adv. Mater.*, 2003, **15**, 411.
- D. A. Rani, D. D. Jayaseelan and F. D. Gnanam, *J. Eur. Ceram. Soc.*, 2001, **21**, 2253.